

Eddy Current Tomography in Cylindrical Geometry

D. Prémel and A. Mohammad-Djafari

Laboratoire des Signaux et Systèmes (CNRS-ESE-UPS), École Supérieure d'Électricité

Plateau de Moulon, 91192 Gif-sur-Yvette Cedex, France.

Abstract—A tomographic approach is proposed for the inhomogeneities imaging in conductive media. We propose a linear discrete model for the resolution of the Forward problem and a Bayesian probabilistic approach for the resolution of the inverse problem. Some results (simulated and real data) are presented to show the efficiency of the proposed method in spite of the modelization errors due to the Born approximation for linearizing the problem. Our specific application concerns the Eddy current non-destructive evaluation of pipes.

I. INTRODUCTION

This paper concerns the implementation of a tomographic imaging procedure to invert eddy current data. Eddy current imaging methods consist of dividing the defective region using a regular mesh and then considering the non-destructive evaluation (NDE) problem in the same way as that of tomographic reconstruction problem for heterogeneous media. In opposition to the qualitative imaging methods which consist of reconstructing the flaw's contours by estimating the density of the induced currents [5], our objective is to reconstruct directly the quantitative map of the relative conductivity of the flawed region (object). This imaging approach requires, first, to construct a model (**Forward** problem) which can be able to regenerate the responses supplied by the sensors. This model must be constructed faithfully to be as simple as possible. Next step is the experimental design to make and to measure the data (**instrumentation**). Finally, an image of the interested region must be reconstructed from the measured data (**inverse** problem).

These three problems are commonly not independent and the resolution of the inverse problem requires to solve many times the Forward problem. Unfortunately, forward models are inherently nonlinear, because they involve two linear coupled integral equations where the observed data are related, by an integral equation, to the products of two unknowns, the flaw conductivity and the true electric field within the flawed region. The Born approximation is therefore introduced to linearize the problem by assuming that the perturbation of the electric field within the flawed region is small. In this paper, we first derive such a linearized model which makes a relatively good compromise between the fidelity to measured data and the simplicity of the model. Next, we propose an inversion method to reconstruct the object. We show in particular the way we have introduced an *a priori* information by using a Bayesian approach in order to obtain a satisfactory solution in spite of the modelization errors inherently due to the Born approximation. Some simulation results are presented to show the

efficiency of the proposed method. First, we compare our results with real data and with the results obtained by a finite element method. Then, we present some reconstructed images of artificial objects from real data.

II. RESOLUTION OF THE FORWARD PROBLEM

Let us consider an anomalous region within the wall of a cylindrical tube, with conductivity σ_0 and permeability μ_0 and consider a flaw which has axial symmetry. The flawed region is assumed to have the same permeability μ_0 but different conductivity $\sigma(r, z)$. An exciting coil and a probe coil are in the interior of the tube and are coaxial with it. The exciting coil provides eddy current in the tube wall and the probe coil measures the voltages induced in the sensing coil. Given the object function $f(r, z) = (\sigma_0 - \sigma(r, z))/\sigma_0$, the determination of the responses of the sensing coils requires the followings steps:

1. Calculate the field $E_{20}(\vec{r})$ inside the wall of the tube produced by the exciting coil considering the flaw absent:

$$E_{20}(\vec{r}) = j\omega\mu_0 \int_{\text{inductor}} G_{21}(\vec{r}, \vec{r}') J_0(\vec{r}') d\vec{r}', \quad (1)$$

where $J_0(\vec{r}')$ represents the induced current by the source.

2. Calculate the field $E_2(\vec{r})$ inside the tube wall when the flaw is present:

$$E_2(\vec{r}) = E_{20}(\vec{r}) + j\omega\mu_0\sigma_0 \int_D G_{22}(\vec{r}, \vec{r}') E_2(\vec{r}') f(\vec{r}') d\vec{r}'. \quad (2)$$

3. Calculate $e(\omega, z)$ which is induced in the probe coil:

$$e(\omega, z) = \int_D H(\omega, z; \vec{r}') \sigma_0 f(\vec{r}') E_2(\vec{r}') d\vec{r}', \quad (3)$$

where the function $H(\omega, z; \vec{r}')$ is given by

$$H(\omega, z; \vec{r}') = -j\omega\mu_0 2\pi n_s \int_{\text{probe}} G_{12}(\vec{r}, \vec{r}') d\vec{r}'. \quad (4)$$

In these equations, $G_{21}(\vec{r}, \vec{r}')$ and $G_{22}(\vec{r}, \vec{r}')$ are the Green's functions, n_s denote the whirls density and ω is the frequency of the exciting source. We have considered three regions of interest: the interior of the tube R_1 , the tube's wall R_2 , and the exterior to the tube R_3 .

The inverse problem which consists in reconstructing the object function $f(\vec{r})$ from the measured data $e(\omega, z)$ now appears like a bi-linear inverse problem. To linearize and to decouple the equation (2) and (3) one can use the Born

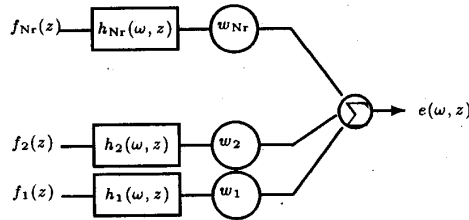
approximation. Within this approximation and for a two dimensional problem, the relation between the measured data and the object function becomes:

$$e(\omega, z) = \int_D H(\omega, z; r', z') \sigma_0 f(r', z') E_{20}(r', z') r' dr' dz'. \quad (5)$$

The function $H(\omega, z; r', z')$ includes the geometry of the probe coil while the incident field $E_{20}(r', z')$ includes the geometry of the exciting coil. The next step consists of discretizing this linear integral equation with rectangular basis functions and Dirac weight functions (point-matching). The flawed region is partitioned into k layers ($1 \leq k \leq N_r$), defining the successive lines $f_k(z) = f(r_k, z)$ of the image $f(r, z)$. The measured data $e(\omega, z)$ are, finally, related to the object function by the following relation:

$$e(\omega, z) = \sum_{k=1}^n w_k f_k(z) * h_k(\omega, z) + b(\omega, z) \quad (6)$$

where $*$ means the convolution operator and w_k is related to the incident field values $E_{20}(r_k)$ at each layer k . The point spread functions $h_k(\omega, z)$ to the sensor are defined from the Green's functions depending only to the geometry of the measurement system and the frequency ω of the exciting waves. This equation shows the dependence of $e(\omega, z)$ and $h_k(\omega, z)$ on the frequency ω , whereas $f_k(z)$ is independent of ω . By acquiring data at several frequencies and writing down equation (6) for each frequency, we obtain a system of N_f equations that we call the multifrequency linear model. For each frequency we have:



In our application we have chosen four frequencies occurring in octave steps. This choice improves the condition number of the resulting linear system due to the physical phenomenon "skin effect" which contributes to confine high frequency eddy currents near to the exciting source. Furthermore, the inverse problem is underdetermined since the number of measurement data is smaller than the number of unknowns. For these reasons, we have to complete the information provided by the data with *a priori* information on the object $f(r, z)$. One way to achieve this is to adopt a Bayesian approach.

III. A BAYESIAN APPROACH FOR THE INVERSE PROBLEM

The observation model (6) is given by a set of linear integral equations whose kernels are translation invariant along the measuring axis. When discretized we have:

$$\mathbf{y} = \mathbf{A} \mathbf{x} + \mathbf{b} \quad (7)$$

where \mathbf{A} is a known attenuating matrix whose components depend only on the geometry of the experimental system

through the functions $h_k(\omega, z)$. \mathbf{x} is a vector whose components represent the unknown parameters to estimate (the pixel values of the image $f(r, z)$). \mathbf{y} is a vector whose components are the samples of the measured data $e(\omega, z)$ collected from several frequencies. \mathbf{b} is a vector whose components represent both the measurement noise and any other unmodeled error like quadrature errors resulting from the discretization and model approximation errors. In this paper, we propose a Bayesian approach which is based on the use of *a priori* information on \mathbf{x} and \mathbf{b} and involves the following steps [3,2]:

1. Assign a probability law $p(\mathbf{x})$ to the unknown parameters \mathbf{x} to translate our *a priori* knowledge about them.
2. Assign a conditional probability law $p(\mathbf{y}|\mathbf{x})$ to the measured data to translate our uncertainty on the observation model and on the noise that corrupts the measured data.
3. Use the Bayes rule to obtain the *a posteriori* distribution $p(\mathbf{x}|\mathbf{y})$ which completely sums up all the knowledge we can have about the object \mathbf{x} :

$$p(\mathbf{x}|\mathbf{y}) = p(\mathbf{y}|\mathbf{x})p(\mathbf{x})/p(\mathbf{y}) \quad (8)$$

4. Use a decision rule to attribute a value to each pixel. There are three classical estimators: the maximum *a posteriori* (MAP), the posterior mean (PM) and the marginal maximum *a posteriori* (MMAP). This choice is often translated into the choice of a cost function $C(\mathbf{x}^*, \mathbf{x})$ and the solution $\hat{\mathbf{x}}$ is obtained by minimizing its mean value.

Several difficulties still remain. First, how to assign the probability law $p(\mathbf{x})$ to the unknown parameters because the *a priori* knowledge is not given to us directly in a probabilistic terms. Second, the choice of a cost function is not obvious. In the next section, we describe the choices we have made to implement this inversion method in our eddy current imaging context.

IV. THE PROPOSED METHOD

A. Assigning the *a priori* law $p(\mathbf{x})$

To assign $p(\mathbf{x})$, we have to translate the *a priori* knowledge that we have about the solution in probabilistic terms. If the *a priori* knowledge can be written down as some constraints on $p(\mathbf{x})$, the Maximum Entropy (ME) principle can be used. In practical applications, we don't have such constraints, so we often translate constraints such as positivity, or roughness of the desired solution to choose a family of laws which are determined by some hyperparameters. These parameters may be fixed in advance or may be estimated from data in the same time that the solution. In our case, the image represents the values of the relative conductivity $f(r, z) = (\sigma_0 - \sigma(r, z))/\sigma_0$ at each pixel position. These values are included in the interval $[0, 1]$. Furthermore, most of these pixel values are close to zero (homogeneous region $f(r, z) = 0$) while the flawed region is almost constituted by air ($f(r, z) = 1$). We translated these information by using a Beta probability distribution

function for the pixel values.

$$\begin{aligned} p(x_i) &= \frac{1}{Z} x_i^{-\lambda} (1-x_i)^{-\mu} \\ &= \frac{1}{Z} \exp[-\lambda \log x_i - \mu \log(1-x_i)], \end{aligned} \quad (9)$$

where Z is the normalization constant. This prior law favors the pixel values around 0 and 1 without excluding the intermediate values which represent the materials which are less conductive than the homogeneous region and which are buried in the homogeneous region. The parameters λ and μ can be adjusted to take account of the expected nature and the relative size of the flaw buried into the homogeneous region.

We have also assumed that the pixels are *a priori* independent. So $p(\mathbf{x})$ can be written down in the following expression:

$$p(\mathbf{x}) = \frac{1}{Z^N} \exp \left[-\lambda \sum_{i=1}^N \log x_i - \mu \sum_{i=1}^N \log(1-x_i) \right]. \quad (10)$$

B. Assigning the conditional probability law $p(\mathbf{y}/\mathbf{x})$

When the noise \mathbf{b} is *a priori* assumed to be white, with a covariance matrix $\mathbf{W} = \text{diag} \left[\frac{1}{\sigma_1^2}, \dots, \frac{1}{\sigma_M^2} \right]$, the ME principle gives us a Gaussian distribution:

$$p(b_j) = \mathcal{N}(0, \sigma_j^2), j \in \{1, 2, \dots, M\},$$

where M is the number of samples of the measured signal. Then, using the observation model (7), we obtain:

$$p(\mathbf{y}/\mathbf{x}) \propto \exp[-Q(\mathbf{x})] \text{ with } Q(\mathbf{x}) = (\mathbf{y}-\mathbf{A}\mathbf{x})^t \mathbf{W} (\mathbf{y}-\mathbf{A}\mathbf{x}). \quad (11)$$

C. Calculating the a posteriori law $p(\mathbf{x}/\mathbf{y})$

By substituting the equation (10) and (11) into (8), we obtain:

$$p(\mathbf{x}/\mathbf{y}) \propto \exp[-J(\mathbf{x})] \text{ with } J(\mathbf{x}) = Q(\mathbf{x}) + \lambda H(\mathbf{x}) + \mu S(\mathbf{x}), \quad (12)$$

where the two functions $H(\mathbf{x})$ and $S(\mathbf{x})$ are defined by the following relations:

$$H(\mathbf{x}) = \sum_{i=1}^N \log(x_i) \quad \text{and} \quad S(\mathbf{x}) = \sum_{i=1}^N \log(1-x_i). \quad (13)$$

D. Choice of the cost function

When $p(\mathbf{x}/\mathbf{y})$ calculated, in general, we need to summarize it by attributing an optimal value to each pixel. One can choose as the optimal solution $\hat{\mathbf{x}}$ the mode, the mean or the mode of the marginal $p(x_i/\mathbf{y})$. This choice is often translated into the choice of a cost function $C(\mathbf{x}^*, \mathbf{x})$ and the solution $\hat{\mathbf{x}}$ is obtained by minimizing its mean value

$$\hat{\mathbf{x}} = \arg \min_{\mathbf{x}} \left\{ \int C(\mathbf{x}^*, \mathbf{x}) p(\mathbf{x}^*/\mathbf{y}) d\mathbf{x}^* \right\}. \quad (14)$$

The choice is guided by the fact that it is necessary to make a compromise between several practical constraints

like: the complexity of the implementation, the quantity of calculations which are required in order to obtain an explicit solution. We have adopted the MAP solution:

$\hat{\mathbf{x}} = \arg \max_{\mathbf{x}} \{p(\mathbf{x}/\mathbf{y})\}$ which can be interpreted as the choice of a zero-one cost function. We have adopted it because it leads to the simplest implementation and, practically, it leads to a satisfactory solution.

E. Resulting optimization problem

With this choice, the solution of the inverse problem is obtained by minimizing a mixed criterion:

$$\hat{\mathbf{x}} = \arg \min_{\mathbf{x}} \{J(\mathbf{x}) = Q(\mathbf{x}) + \lambda H(\mathbf{x}) + \mu S(\mathbf{x})\}. \quad (15)$$

In a related paper [3], we have presented this approach and shown that one can give a regularization interpretation to this criterion where the two functions $H(\mathbf{x})$ and $S(\mathbf{x})$ appear as regularization functionals and λ and μ as regularization parameters.

If λ and μ are fixed in advance, then $J(\mathbf{x})$ is a convex function of \mathbf{x} and therefore its optimization does not induce any particular difficulty. Any gradient algorithm can then be used to obtain the solution. We have implemented a modified conjugate gradient algorithm which, in each iteration, forces the values of $\hat{\mathbf{x}}$ to be in the interval $[0, 1]$.

IV. NUMERICAL RESULTS

To validate our forward model and our inversion method artificial axisymmetric flaws in the internal or in the external faces of a copper tube are constructed. This tube has an inner radius of 9mm and an outer radius of 10mm. The flaws are 0.3mm deep and have a length of 5mm.

Using this tube, the experimental data has been gathered for five frequencies (1, 2, 4, 8, 16kHz). Then, a comparison is done between these experimental data and those obtained by using our simplified forward method, as well as, with those obtained by a finite element method who does not need the Born approximation.

In Fig. 1 and Fig. 2 we present these results. In these figures the simulation results obtained by the proposed method are noted (LSS) and those obtained by a finite element (FE) method are noted (ECL) and the experimental data are noted (CEA). Two commonly used representations in non-destructive testing are used to show these data. The first is the variation of the amplitude of the data as a function of z . The second is the variation of the imaginary part as a function of the real part of the data. Fig. 1 corresponds to an external flaw and Fig. 2 to an internal flaw.

Comparing the results obtained by the proposed method to those of the FE method, we can see that for an external flaw the first one gives a better restitution of the phase variations and second one gives a better restitution of the amplitude variations. For an internal flaw these are reversed. However these results show a good concordance between the experimental data and those provided by the proposed model.

In Fig. 3 the inversion results (reconstructed objects) we have obtained are, respectively, presented by a non-

regularized method, a quadratic regularization method, and the proposed method. All these images are obtained from the real data. The reconstructed objects by the proposed method are better than the others. It is not surprising because the latter take account of a pertinent *a priori* information which improves naturally the results.

V. CONCLUSIONS

The main objective of this paper was to present a procedure for the imaging of conductive media and which allows to be applied efficiently for eddy current non-destructive evaluation. The Bayesian approach we have described have permitted us to introduce an *a priori* information which is a relevant and specific one for our application. Furthermore, contrary to quadratic regularization methods which are usually used by other authors [4,6], the regularization functionals we have proposed guarantee the positivity of the solution. In particular, the reconstructed objects obtained from real data show that the proposed method seems to be very robust relative to modelization errors. Two extensions for this work are presently doing: the estimation of the regularization parameters λ and μ from the data [3,7] and the introduction of other *a priori* information in order to take account of *a priori* known correlation between the adjacent pixel values using a Markov model [8].

VI. ACKNOWLEDGMENT

The authors wish to thank R. Besnard¹ and N. Burais² for providing us, respectively, the experimental data and the simulated data by a finite element method.

REFERENCES

- [1] D. Prémel, A. Mohammad-Djafari, G. Demoment, B. David, "Tomographie par courants de Foucault," *Actes du 1er Congrès COFREND sur les essais non destructifs*, Nice 6-9 Novembre 1990.
- [2] A. Mohammad-Djafari and G. Demoment, "Image restoration and reconstruction using entropy as a regularization functional," *Maximum Entropy and Bayesian Methods in Science and Engineering*, edited by Kluwer Academic Publishers, Vol. 2, pp:341-355, 1988.
- [3] D. Prémel, A. Mohammad-Djafari, B. David, "Imagerie de milieux conducteurs par courants de Foucault," *Actes du 19ième Colloque GRETSI*, Juan-les-Pins, 16-20 Septembre 1991.
- [4] H.A. Sabbagh and L.D. Sabbagh, "Development of a system to invert eddy-current data and reconstruct flaws," *International advances in nondestructive testing*, W.J. McGonnagle, Ed. New York: Gordon and Breach, pp: 267-305, 1984.
- [5] R. Zorgati, B. Duchene, D. Lesselier & F. Pons, "Eddy current testing of anomalies in conductive materials, part 1: Qualitative imaging via diffraction tomography techniques", *IEEE Trans. on magnetics*, 27, No. 6, pp. 4416-4437, 1991.
- [6] R. Zorgati, B. Duchene, D. Lesselier & F. Pons, "Eddy current testing of anomalies in conductive materials, part 2: Quantative imaging via deterministic and stochastic inversion techniques", *IEEE Trans. on magnetics*, 28, No. 3, pp. 1850-1862, 1992.
- [7] A. Mohammad-Djafari, "Estimation des hyperparamètres dans une approche bayésienne de la régularisation", *Actes du quatrième colloque GRETSI*, Juan-les-pins, Sept 1993.
- [8] M. Nikolova, A. Mohammad-Djafari and J. Idier, "Inversion of large support ill-conditioned linear operators using a markov model with a line process", *ICASSP-94*, Vol. 5, pp:357-360, 1994.

¹CEA/DTA/CEREM/DPSA/LCME, SACLAY

²LABORATOIRE D'ÉLECTROTECHNIQUE DE LYON - ÉCOLE CENTRALE DE LYON

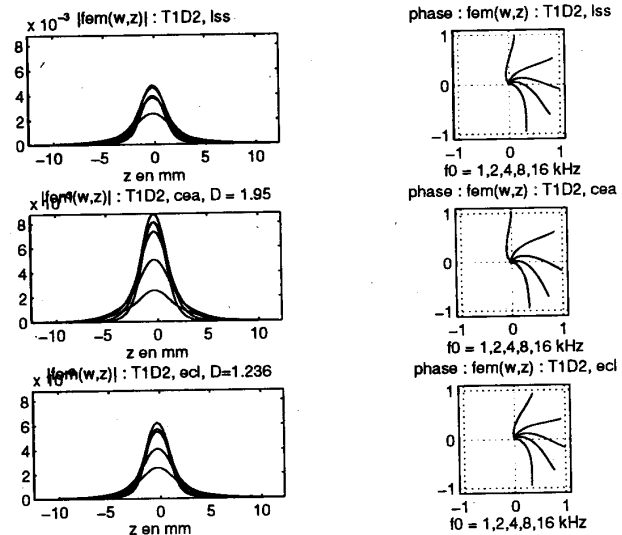


Fig. 1: Validation of the forward model for an external flaw : Comparison between the data obtained by the proposed model (LSS), experimental data (CEA) and the data obtained by a finite element method (ECL).

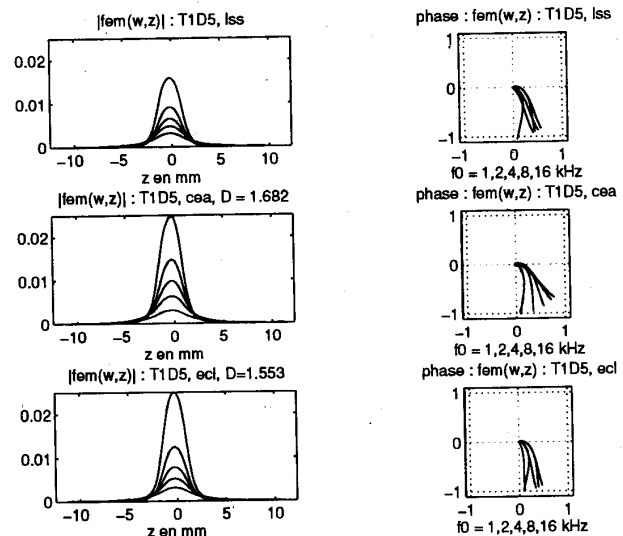


Fig. 2: Validation of the forward model for an internal flaw: a) proposed model, b) experimental data and c) finite element method.

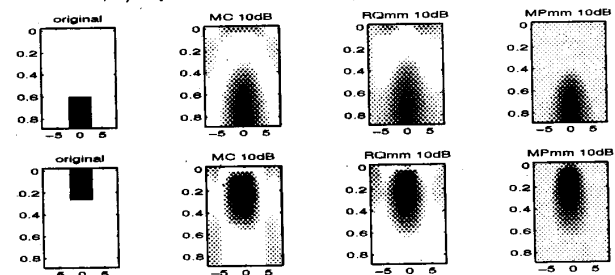


Fig. 3: Validation of the inversion method : Comparison between three reconstruction methods: a least square method (MC), a quadratic regularization method (RQ) and the proposed method.